JACS
JOURNAL OF THE AMERICAN CHEMICAL SOCIETY

COMMUNICATION

pubs.acs.org/JACS

Rapid C−H Bond Activation by a Monocopper(III)−Hydroxide Complex

Patrick J. Donoghue,[†] Jacqui Tehranchi,[†] Christopher J. Cramer,[†] Ritimukta Sarangi,[‡] Edward I. Solomon,[‡,§] and William B. Tolman*[,†]

[†]Department of Chemistry, Center for Metals in Biocatalysis, and Supercomputing Institute, University of Minnesota, 207 Pleasant Street SE, Minneapolis, Minnesota 55455, United States

[‡]Stanford Synchrotron Radiation Lightsource, SLAC National Accelerator Laboratory, Menlo Park, California 94025, United States

[§]Department of Chemistry, Stanford University, Stanford, California 94305, United States

Supporting Information

ABSTRACT: One-electron oxidation of the tetragonal Cu(II) complex [Bu_4N][LCuOH] at −80 °C generated the reactive intermediate LCuOH, which was shown to be a Cu(III) complex on the basis of spectroscopy and theory (L = *N*,*N*′-bis(2,6-diisopropylphenyl)-2,6-pyridinedicarboxamide). The complex LCuOH reacts with dihydroanthracene to yield anthracene and the Cu(II) complex LCu(OH_2). Kinetic studies showed that the reaction occurs via H-atom abstraction via a second-order rate law at high rates (cf. $k = 1.1(1)\ M^{-1}\ s^{-1}$ at −80 °C, $\Delta H^{\ddagger} = 5.4(2)$ kcal mol^{-1}, $\Delta S^{\ddagger} = -30(2)$ eu) and with very large kinetic isotope effects (cf. $k_H/k_D = 44$ at −70 °C). The findings suggest that a Cu(III)−OH moiety is a viable reactant in oxidation catalysis.

Copper−oxygen species are implicated as intermediates in a wide range of oxidation reactions promoted by metalloenzymes,[1] synthetic complexes,[2,3] and materials.[4] Understanding the structures, properties, and reactivities of such species is critical for obtaining mechanistic insights into oxidation catalysis and for developing new, selective catalytic reagents and processes. Efforts to isolate and characterize reactive copper−oxygen intermediates through studies of copper-containing enzymes and synthetic model complexes have led to the identification of several core motifs,[5] exemplified by those shown in Chart 1. Complexes comprising cores **A**−**E** have been well-defined and, as a result, have often been considered as viable oxidants in various catalytic reactions.[6] The monocopper-oxo/oxyl core (**F**) has also been discussed[7] as a candidate capable of attacking hydrocarbon substrates (cf. by peptidylglycine α-hydroxylating monooxygenase[8]), but examples of such species have only been characterized in the gas phase[9] and through theoretical calculations.[8,10] We report herein the preparation and characterization by spectroscopy and theory of a new type of copper−oxygen intermediate containing a hydroxo-copper(III) core (**G**), which formally may be considered as a protonated version of **F**.[11] The complex comprising **G** rapidly abstracts hydrogen atoms from the C−H bonds of dihydroanthracene, thus providing a key precedent for the possible involvement of **G** in oxidation catalysis.

Chart 1. Copper Oxygen Intermediate Cores

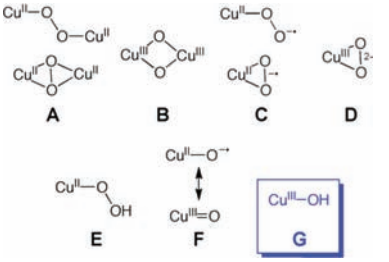

As starting material we used the tetragonal copper(II) complex LCu(CH_3CN) (**1**, L = *N*,*N*′-bis(2,6-diisopropylphenyl)-2,6-pyridinedicarboxamide, Figure 1), for which we report a new X-ray crystal structure (Figure S1). Treatment of **1** dissolved in THF or suspended in Et_2O with a solution of Bu_4NX (X = Cl or OH) in MeOH yielded deep green or blue [Bu_4N][LCuX] ([Bu_4N][**2**] or [Bu_4N][**3**]), respectively. Both products were isolated as solids and characterized by UV−vis, FTIR, and EPR spectroscopy, and CHN analysis.[12] Notable data include a sharp ν(OH) at 3628 cm^{-1} in the FTIR spectrum (nujol) of [Bu_4N][**3**] and essentially axial EPR signals for both complexes consistent with tetragonal Cu(II) species (Figures S2−S3 and Table S1 in the Supporting Information). Crystals of both complexes suitable for characterization by X-ray diffraction were obtained by metathesis with PPNCl (Figures 1 and S4, Table 1). While the structure of [PPN][**2**] is straightforward, in [PPN][**3**] the longer than expected Cu−O distance of 1.947(2) Å[13] led us to suspect that the crystals were a compositionally disordered[14] mixture of the chloride and hydroxide complexes, with the chloride ligand having been derived from displacement of hydroxide by the added PPNCl. Consistent with this notion, the UV−vis spectral features for [Bu_4N][**3**] in THF cleanly converted to those for [Bu_4N][**2**] upon addition of Bu_4NCl (1 equiv from titration experiments; Figure S5). In addition, comparison of UV−vis spectra of crystals of [PPN][**3**] (3 batches) to those of pure [Bu_4N][**2**] and [Bu_4N][**3**] indicated chloride contamination levels of 22−28%. Finally, DFT (*m*PW) calculations were performed for $\mathbf{2}^-$ and $\mathbf{3}^-$ that yielded minimum energy

Received: August 19, 2011
Published: October 17, 2011

dx.doi.org/10.1021/ja207882h | *J. Am. Chem. Soc.* 2011, 133, 17602–17605

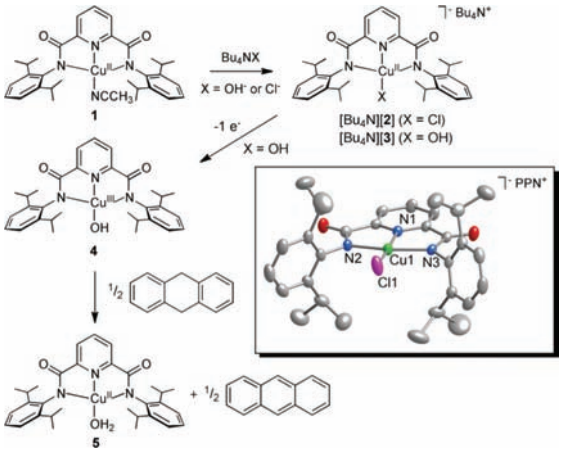

Figure 1. Complexes and reactions studied in this work, with a representation of the anionic portion of the X-ray crystal structure of [PPN][**2**] shown in the box as 50% thermal ellipsoids (H-atoms omitted for clarity).

Table 1. Selected Interatomic Distances for 2^- and 3^- from X-ray Crystallography and *m*PW Calculations[a]

	2^-		3^-	
	X-ray	*m*PW	X-ray	*m*PW
Cu−N1	1.926(2)	1.961	1.920(2)	1.947
Cu−N2	1.992(2)	2.073	1.996(2)	2.078
Cu−N3	1.993(2)	2.073	2.010(2)	2.080
Cu−X[b]	2.1842(8)	2.216	1.9465(19)	1.863
Cu−N/O (avg)	1.97	2.04	1.97	1.99

[a] Distances in Å; X-ray data for PPN^+ salts. [b] For 2^-, X = Cl; for 3^-, X = OH.

structures with Cu−N bond distances somewhat longer than those measured by X-ray crystallography (Table 1), as is common for *m*PW calculations with bulky ligands.[15] However, a significantly shorter Cu−OH distance was calculated for 3^- (1.863 Å) than was observed in the X-ray crystal structure (1.9465(19) Å). EXAFS data collected for [Bu_4N][**3**] (powder, not exposed to PPNCl) were best fit with 4N/O donors[16] and average metal−ligand distances of 1.95 Å (Figures S6 and S7), slightly shorter than those determined by X-ray crystallography and *m*PW (Table 1). The EXAFS data collected for [Bu_4N][**2**] were best fit with 3 N/O donors averaging 1.98 Å and one Cl donor at 2.21 Å, which is also in good agreement with the X-ray crystal structure and *m*PW calculations. Taken together, the data support the hypothesis of a compositionally disordered X-ray crystal structure for [PPN][**3**] with a Cu−O distance that is overestimated by ∼0.1 Å.

The tetragonal Cu(II) complex [Bu_4N][**3**] exhibits a pseudoreversible oxidation in acetone solution (0.1 M Bu_4NPF_6) at room temperature with $E_{1/2}(3^-) = -0.076$ V vs Fc^+/Fc (Figure S11). Chemical oxidation of [Bu_4N][**3**] in acetone was performed using $Fc^+PF_6^-$ at −80 °C,[17] which provided a deeply colored purple solution characterized by an intense low energy electronic absorption feature with $\lambda_{max}(\varepsilon)$ = 540 nm (∼12 400 M^{-1} cm^{-1}) (Figure 2). The solutions were EPR silent. The

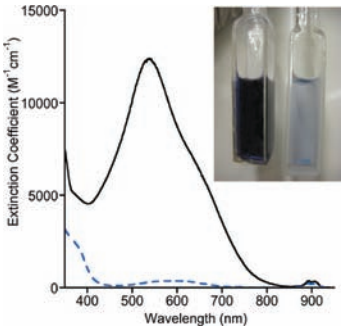

Figure 2. UV−vis spectra of [Bu_4N][**3**] (blue dashed line, right cuvette in photograph) and **4** (solid black line, left cuvette in photograph) in acetone at −80 °C.

Table 2. Selected Structural Parameters for 4 from *m*PW Calculations[a]

	singlet	triplet
Cu−N1	1.872	1.964
Cu−N2	1.952	2.106
Cu−N3	1.961	2.106
Cu−O	1.810	1.844
Cu−N/O (avg)	1.90	2.01

[a] All distances in Å.

absorption features decayed within minutes upon warming to −60 °C. Titration experiments monitored by UV−vis spectroscopy (Figure S12) showed that the oxidation reaction required 1 equiv of oxidant to reach completion. Reduction of this species with 1 equiv of decamethylferrocene (Fc*) added to the chilled solution yielded UV−vis features consistent with **3** and Fc^{*+} (Figures S13). These data are consistent with a reversible one-electron process that generates LCuOH (**4**, Figure 1).

Lacking crystals suitable for X-ray crystallography, we turned to DFT calculations and X-ray absorption spectroscopy to further evaluate the nature of **4**. The one-electron oxidation of 3^- could conceivably result in (a) a metal-based oxidation to yield a Cu(III) species or (b) a ligand-based oxidation to yield a Cu(II)-ligand radical. A Cu(III) species should be a singlet whereas a Cu(II)-ligand radical could be either a triplet or an open-shell singlet. Starting from optimized *m*PW structures of 3^-, a closed-shell singlet structure for **4** was located easily. This oxidized singlet maintained the square-planar geometry and symmetry elements identified in its Cu(II) precursor (C_s). Consistent with the singlet Cu(III) formulation, and in agreement with EXAFS results (see below), upon oxidation of 3^- to **4** the copper−ligand bonds contract; the average Cu−N bond shortens by 0.08 Å, and the Cu−N/O bond average shortens by 0.09 Å (Table 2). Finally, the results of gas phase time dependent DFT (TD B98) calculations for the singlet of **4** match well with the experimentally observed UV−vis features (Figure S14): the singlet wave function for **4** was calculated to have a single transition at 589 nm (2.10 eV), within 0.2 eV of the observed transition at 540 nm (2.30 eV). The dominant one-electron excitation in this transition, with a weight of about 67%, is from an orbital with largely ligand (L) π-character to one largely comprised of the Cu $d_{x^2-y^2}$ (Figure S15). In sum, calculations support a singlet Cu(III) formulation for **4**.

dx.doi.org/10.1021/ja207882h |*J. Am. Chem. Soc.* 2011, 133, 17602–17605

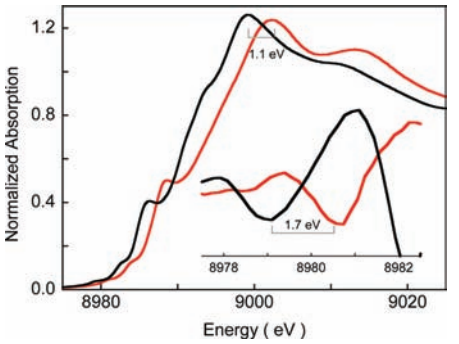

Figure 3. Normalized Cu K-edge XAS spectra of $[Bu_4N][\mathbf{3}]$ (black) and **4** (red). The inset shows the second derivative spectra of the pre-edge region showing the shift on going from $[Bu_4N][\mathbf{3}]$ to **4**.

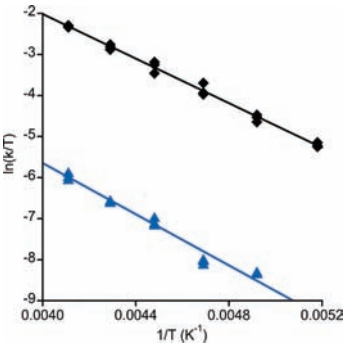

Figure 4. Plots of $\ln(k/T)$ vs $1/T$ (where k = second-order rate constant, T = temperature in K) for the reaction of **4** with DHA (black diamonds) or DHA-d_4 (blue triangles). The shown linear fits were used to calculate the activation parameters listed in the text via the Eyring equation (R = 0.997 and 0.985, respectively).

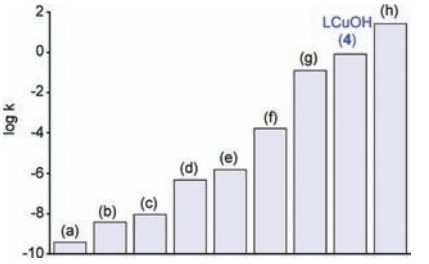

Figure 5. Comparison of the second-order rate constants (k in units of M^{-1} s^{-1}, on a logarithmic scale) for oxidation of DHA at −80 °C by selected copper, iron, and manganese complexes with that of LCuOH (**4**). For (g) and (h), reported rate constants were used; for (a)−(f), the rate constants were calculated using the Eyring equation from the reported activation parameters. (a) $[Cu^{III}(Pre)]^+$ (ref 20); (b) $[Fe^{III}(Hbim)(H_2bim)_2]^{2+}$ (ref 21); (c) $[Fe^{III}(PY5)OH]^{2+}$ (ref 22); (d) $[Mn^{III}(H3buea)O]^-$, $[MnO_4]^-$ (refs 23, 24); (e) $[Mn^{III}(PY5)OH]^{2+}$ (ref 25); (f) $[Mn^{IV}(H3buea)O]^-$ (ref 23); (g) $[L'(CH_3CN)Fe^{IV}O]^{2+}$ (ref 26); and (h) $[L'Fe^{III}(OH)(\mu\text{-}O)(L')Fe^{IV}O]^{2+}$ (ref 26). Abbreviations: Pre = 3,9-dimethyl-4,8-diazaundecane-2,10-dionedioximate, H_2bim = 2,2′-bi-imidazoline, PY5 = 2,6-bis(bis(2-pyridyl)methoxymethane)pyridine, H3buea^{3-} = triply deprotonated form of tris[(*N*′-*tert*-butylureayl)-*N*-ethylene]amine, L′ = tris((4-methoxy-3,5-dimethylpyridin-2-yl)methyl)amine.

Consistent with this conclusion, structures corresponding to a ligand-based oxidation were more difficult to locate by *m*PW. Thus, attempts to identify an open-shell singlet via a broken-symmetry formalism for **4** converged to closed-shell singlet solutions. A triplet structure can be located but is energetically disfavored relative to the closed-shell singlet by 19.0 kcal/mol. Metal−ligand bond distances calculated for the triplet also are relatively unchanged relative to those calculated for the precursor $\mathbf{3}^-$, in contrast to the EXAFS results (see below). Thus, the triplet **4** actually has a slightly longer average Cu−N/O bond length than the starting complex $\mathbf{3}^-$ (2.01 vs 1.99 Å). Finally, TD B98 results for the triplet included several transitions in the near-IR range that were not observed experimentally.

Cu K-edge XAS data provide direct experimental evidence for the Cu(III) formulation of **4**. As shown in Figure 3, the Cu K pre-edge energy position of **4** is shifted ∼1.7 eV to higher energy relative to that of the Cu(II) complex $[Bu_4N][\mathbf{3}]$, indicating one-electron metal-based oxidation with an associated increase in ligand field strength of the Cu center. A shift in the rising edge by ∼1.1 eV is also observed on going from $[Bu_4N][\mathbf{3}]$ to **4**, reflecting the increase in the effective nuclear charge on Cu in **4**.[18] The EXAFS data (Figures S6 and S8, Table S3) provide further confirmation of the Cu(III) nature of **4**. Fits to the data show an ∼0.1 Å shortening of the first shell Cu−O/N bond distances in **4** (4 Cu−N/O at 1.86 Å) relative to $[Bu_4N][\mathbf{3}]$ (4 Cu−N/O at 1.95 Å), typical for oxidation of a Cu(II) to a Cu(III) complex.

Inspired by reports of C−H bond activation by Mn(III), Mn(IV), and Fe(III) hydroxide complexes,[19] we examined the reactivity of **4** with dihydroanthracene (DHA), a commonly studied substrate useful for comparison purposes. The UV−vis features of **4** smoothly decayed upon introduction of 0.5 equiv of DHA to acetone solutions at low temperature, concomitant with the growth of bands due to the formation of anthracene (85% yield by GC/MS). The final inorganic product was determined to be the Cu(II) complex $LCu(OH_2)$ (**5**, Figure 1) on the basis of comparison of the UV−vis spectrum to that of independently synthesized material, which was fully characterized, including by X-ray crystallography (Figure S16). The UV−vis features of **4** decayed according to pseudo-first-order kinetics when the reaction was performed with excess DHA (10−40 equiv), and a plot of k_{obs} vs [DHA] was linear with an intercept that corresponded to the self-decay rate (Figures S17 and S18). These data indicate an overall second-order rate law $-d[\mathbf{4}]/dt = k[\mathbf{4}][DHA]$. A very large kinetic isotope effect (k_H/k_D) of 44 at −70 °C was observed when the reaction was performed with DHA-d_4, and the temperature dependence of this effect was evaluated by an Eyring analysis (Figure 4, Table S4); apparent $\Delta H^{\ddagger}_H$ = 5.4(2) kcal mol^{-1}, $\Delta S^{\ddagger}_H$ = −30(2) eu, $\Delta H^{\ddagger}_D$ = 6.2(3) kcal mol^{-1}, $\Delta S^{\ddagger}_D$ = −34(3) eu. Based on these parameters, the KIE was calculated to be 29 at 25 °C, well beyond the semiclassical limit. Finally, we note that **4** reacted essentially instantaneously at −80 °C with 2,4,6-tri-*tert*-butylphenol to yield the phenoxyl radical (UV−vis, EPR). Together, the reactivity and kinetic data support a mechanism for oxidation of DHA to anthracene that involves rate-determining H-atom abstraction by the Cu(III)−OH moiety, with a tunneling contribution being a reasonable rationale for the larger than semiclassically predicted k_H/k_D values.

The second-order rate constants for reactions of selected relevant Cu(III) or metal-oxo or −hydroxo complexes with DHA at −80 °C are compared to that of **4** in Figure 5.[20−26] The rate of H-atom abstraction from DHA by LCuOH is significantly faster than most other nonheme iron (b,c,g), manganese (d−f), and copper (a) reagents and is comparable to a recently reported

dx.doi.org/10.1021/ja207882h |*J. Am. Chem. Soc.* 2011, 133, 17602–17605

high-spin Fe(III)Fe(IV)-oxo complex (h). While not as intrinsically reactive as the (P^+)Fe(IV)═O intermediate (compound I) in cytochrome P450,[27] the high rate for DHA oxidation by **4** is nonetheless extraordinary in the context of known oxidizing capabilities of copper−oxygen species.[5,7,28] While further work is necessary to understand the basis for this reactivity, we speculate that the high basicity of the hydroxide group is a key factor in view of the fact that the potential for the $\mathbf{3}^-/\mathbf{4}$ couple is modest (−0.076 V vs Fc^+/Fc).[29] Similar arguments have been advanced to rationalize observed rates of H-atom transfer by Mn-oxo.[30,31] and Fe(IV)-imido[32] complexes, as well as cuprous oxide surfaces.[33] The relatively minor structural differences (overall geometry, metal−ligand bond distances) between **4** and **5** may also result in a small reorganization energy that could contribute to a high reaction rate.[34]

In summary, we have prepared a new type of copper−oxygen intermediate and shown through theory and experiment that it is best described as a singlet Cu(III)−OH complex. High rates of H-atom abstraction from phenols and DHA by this complex were observed, indicating that such a species should be considered as a viable intermediate in catalytic oxidation reactions.

■ ASSOCIATED CONTENT

Supporting Information. Experimental details, including characterization data, spectra, X-ray structure drawings, kinetic plots and tables, and calculation protocols and results (PDF) and CIFs. This material is available free of charge via the Internet at http://pubs.acs.org.

■ AUTHOR INFORMATION

Corresponding Author
wtolman@umn.edu

■ ACKNOWLEDGMENT

This research was supported by the NIH (Grants R37-GM47365 to W.B.T.; DK-31450 to E.I.S.) and the NSF (CHE-0952054 to C.J.C.). SSRL operations are funded by the Department of Energy, Office of Basic Energy Sciences. The SSRL Structural Molecular Biology program is supported by the National Institutes of Health, National Center for Research Resources, Biomedical Technology Program, and the Department of Energy, Office of Biological and Environmental Research. This publication was made possible by Award P41 RR001209 from the National Center for Research Resources (NCRR), a component of the National Institutes of Health (NIH).

■ REFERENCES

(1) Klinman, J. P. *Chem. Rev.* **1996**, *96*, 2541–2561. Solomon, E. I.; Sundaram, U. M.; Machonkin, T. E. *Chem. Rev.* **1996**, *96*, 2563–2605.
(2) Díaz-Requejo, M. M.; Pérez, P. J. *Chem. Rev.* **2008**, *108*, 3379–3394.
(3) Que, L., Jr.; Tolman, W. B. *Nature* **2008**, *455*, 333–340.
(4) Woertink, J. S.; Smeets, P. J.; Groothaert, M. H.; Vance, M. A.; Sels, B. F.; Schoonheydt, R. A.; Solomon, E. I. *Proc. Natl. Acad. Sci. U.S.A.* **2009**, *106*, 18908–18913.
(5) Lewis, E. A.; Tolman, W. B. *Chem. Rev.* **2004**, *104*, 1047–1076. Mirica, L. M.; Ottenwaelder, X.; Stack, T. D. P. *Chem. Rev.* **2004**, *104*, 1013–1045. Hatcher, L.; Karlin, K. D. *J. Biol. Inorg. Chem.* **2004**, *9*, 669–683. Itoh, S. *Curr. Opin. Chem. Biol.* **2006**, *10*, 115–122.
(6) For example, see: Itoh, S.; Fukuzumi, S. *Acc. Chem. Res.* **2007**, *40*, 592–600.
(7) Himes, R. A.; Karlin, K. D. *Curr. Opin. Chem. Biol.* **2009**, *13*, 119–131. Hong, S.; Gupta, A. K.; Tolman, W. B. *Inorg. Chem.* **2009**, *48*, 6323–6325 and references cited therein.
(8) Chen, P.; Solomon, E. I. *J. Am. Chem . Soc.* **2004**, *126*, 4991–5000. Evans, J. P.; Ahn, K.; Klinman, J. P. *J. Biol. Chem.* **2003**, *278*, 49691–49698. Yoshizawa, K.; Kihara, N.; Kamachi, T.; Shiota, Y. *Inorg. Chem.* **2006**, *45*, 3034–3041. Crespo, A.; Marti, M. A.; Roitberg, A. E.; Amzel, L. M.; Estrin, D. A. *J. Am. Chem. Soc.* **2006**, *128*, 12817–12828.
(9) Schröder, D.; Holthausen, M. C.; Schwarz, H. *J. Phys. Chem. B* **2004**, *108*, 14407–14416. Dietl, N.; van der Linde, C.; Schlangen, M.; Beyer, M. K.; Schwarz, H. *Angew. Chem., Int. Ed.* **2011**, *50*, 4966–4969.
(10) Yoshihide, N.; Kimihiko, H.; Tetsuya, T. *J. Chem. Phys.* **2001**, *114*, 7935–7940. Decker, A.; Solomon, E. I. *Curr. Opin. Chem. Biol.* **2005**, *9*, 152–163. Gherman, B. F.; Heppner, D. E.; Tolman, W. B.; Cramer, C. J. *J. Biol. Inorg. Chem.* **2006**, *11*, 197–205. Huber, S. M.; Ertem, M. Z.; Aquilante, F.; Gagliardi, L.; Tolman, W. B.; Cramer, C. J. *Chem.—Eur. J.* **2009**, *15*, 4886–4895. Gherman, B. F.; Tolman, W. B.; Cramer, C. J. *J. Comput. Chem.* **2006**, *27*, 1950–1961.
(11) Protonation of a species with core **F** to yield a compound with core **G** has been postulated: Reinaud, O.; Capdevielle, P.; Maumy, M. *J. Chem. Soc., Chem. Commun.* **1990**, 566–568.
(12) See the Supporting Information.
(13) Some reported Cu−OH bond distances in terminal moncopper−hydroxide complexes: (1.878(2) Å) Berreau, L. M.; Mahapatra, S.; Halfen, J. A.; Young, V. G., Jr.; Tolman, W. B. *Inorg. Chem.* **1996**, *35*, 6339–6342.(1.875(2) Å) Lee, S. C.; Holm, R. H. *J. Am. Chem. Soc.* **1993**, *115*, 11789–1198.
(14) Parkin, G. *Chem. Rev.* **1993**, *93*, 887–911.
(15) Cramer, C. J. *Essentials of Computational Chemistry: Theories and Models*, 2nd ed.; Wiley & Sons: New York, 2004; p 291.
(16) Large Debye−Waller factors for this fit are consistent with a spread of Cu−N/O distances, consistent with the X-ray data and DFT calculations.
(17) XAS samples were prepared using $(p\text{-tolyl})_3N^+PF_6^-$.
(18) DuBois, J. L.; Mukherjee, P.; Stack, T. D. P.; Hedman, B.; Solomon, E. I.; Hodgson, K. O. *J. Am. Chem. Soc.* **2000**, *122*, 5775–5787.
(19) Shi, S.; Wang, Y.; Xu, A.; Wang, H.; Zhu, D.; Roy, S. B.; Jackson, T. A.; Busch, D. H.; Yin, G. *Angew. Chem., Int. Ed.* **2011**, *50*, 7321–7324 and references cited therein.
(20) Lockwood, M. A.; Blubaugh, T. J.; Collier, A. M.; Lovell, S.; Mayer, J. M. *Angew. Chem., Int. Ed.* **1999**, *38*, 225–227.
(21) Roth, J. P.; Mayer, J. M. *Inorg. Chem.* **1999**, *38*, 2760–2761.
(22) Goldsmith, C. R.; Stack, T. D. P. *Inorg. Chem.* **2006**, *45*, 6048–6055.
(23) Parsell, T.; Yang, M.; Borovik, A. *J. Am. Chem. Soc.* **2009**, *131*, 2762–2763.
(24) Gardner, K. A.; Kuehnert, L. L.; Mayer, J. M. *Inorg. Chem.* **1997**, *36*, 2069–2078.
(25) Goldsmith, C. R.; Cole, A. P.; Stack, T. D. P. *J. Am. Chem. Soc.* **2005**, *127*, 9904–9912.
(26) Xue, G.; De Hont, R.; Münck, E.; Que, L., Jr. *Nat. Chem.* **2010**, *2*, 400–405.
(27) Rittle, J.; Green, M. T. *Science* **2010**, *330*, 933–937.
(28) Itoh, S. *Curr. Opin. Chem. Biol.* **2006**, *10*, 115–122.
(29) Green, M. T. *Curr. Opin. Chem. Biol.* **2009**, *13*, 84–88.
(30) Prokop, K. A.; de Visser, S. P.; Goldberg, D. P. *Angew. Chem., Int. Ed.* **2010**, *49*, 5091–5095.
(31) Borovik, A. S. *Chem. Soc. Rev.* **2011**, *40*, 1870–1874.
(32) Nieto, I.; Ding, F.; Bontchev, R. P.; Wang, H.; Smith, J. M. *J. Am. Chem. Soc.* **2008**, *130*, 2716–2717.
(33) Reitz, J. B.; Solomon, E. I. *J. Am. Chem. Soc.* **1998**, *120*, 11467–11478.
(34) Mayer, J. M. *Acc. Chem. Res.* **2011**, *44*, 36–46.

■ NOTE ADDED AFTER ASAP PUBLICATION

The values in Table 2 were corrected, to agree with the data discussed in the text, on November 2, 2011.